Supporting Information

Single Photon Emission from a Plasmonic Light Source Driven by a Local Field-Induced Coulomb Blockade

Christopher C. Leon[1,*], Olle Gunnarsson[1,*], Dimas G. de Oteyza[2-4], Anna Rosławska[1,5], Pablo Merino[1,6,7], Abhishek Grewal[1], Klaus Kuhnke[1,*], Klaus Kern[1,8]

[1]Max-Planck-Institut für Festkörperforschung, D-70569 Stuttgart, Germany.

[2]Donostia International Physics Center, E-20018 San Sebastián, Spain.

[3]Centro de Fisica de Materiales, CSIC-UPV/EHU, E-20018 San Sebastián, Spain.

[4]Ikerbasque, Basque Foundation for Science, E-48013 Bilbao, Spain.

[5]present address: Université de Strasbourg, CNRS, IPCMS, UMR 7504, F-67000 Strasbourg, France.

[6]Instituto de Ciencia de Materiales de Madrid, CSIC, c/Sor Juana Inés de la Cruz 3, E-28049 Madrid, Spain.

[7]Instituto de Física Fundamental, CSIC, Serrano 121, E-28006, Madrid, Spain.

[8]Institut de Physique, École Polytechnique Fédérale de Lausanne, CH-1015 Lausanne, Switzerland.

[*]Corresponding Authors: c.leon@fkf.mpg.de, o.gunnarsson@fkf.mpg.de, k.kuhnke@fkf.mpg.de

Model

The C_{60} film is described as a few (n) layers of C_{60} molecules forming a (111) surface whose molecular positions and orientations are obtained from bulk crystalline C_{60}[22]. The film's electronic structure is based on a tight-binding parameterization of $4n$ molecules per unit cell volume that is periodically continued to form an infinite film parallel to the surface. The factor 4 accounts for the four different molecular orientations of C_{60} that are the observed positions found to be frozen in at 4 K, the experimental temperature. One $2p$ orbital is placed on each C atom, pointing radially out from the molecule. The five HOMO (h_u) and three LUMO (t_{1u}) frontier orbitals of each molecule are then constructed from these $2p$ orbitals. The hopping integrals between the $2p$ orbitals are parameterized by fitting them to DFT calculations[9] from which the hopping integrals between the HOMO and LUMO orbitals on different molecules as well as the potential energies of these orbitals are then calculated. This results in a very accurate representation of the LUMO DFT band structure.[9] The electronic structure

calculation of the full film then involves (8 × 4*n*) by (8 x 4*n*) matrices. The factor 8 accounts for the h_u and t_{1u} orbitals of C_{60}.

Electrostatic effects are gradually added to the model, starting with the STM tip being absent. In this context the C_{60} layer is treated as a homogeneous dielectric medium with a dielectric constant of ε=4.4[35] that rests on a perfect metal surface. The C_{60} layer thickness is $na/\sqrt{3}$, where *a* is the C_{60} lattice parameter and the factor $1/\sqrt{3}$ is due to the crystal face being (111). The image charges due to an electron in the LUMO or a hole in the HOMO are now considered. An electron in the LUMO on molecule i feels an image potential $-U_i^{\text{image}}$, while a hole in the HOMO feels the potential $+U_i^{\text{image}}$. The effect of the vacuum-C_{60} and C_{60}-metal interfaces are taken into account using image charges and the appropriate boundary conditions for these interfaces. Image charges are chosen such that the boundary conditions are satisfied for one surface at a time. This approach is iterated until the process converges and the boundary conditions are finally satisfied at both surfaces.

Next, we take the tip into account. The tip is described as a sphere with radius *R* = 1 nm whose surface is a distance *d* away from the vacuum-C_{60} interface. A charge $Q = U_t R$ is added at the sphere's center to obtain the potential U_t at the sphere's surface. Image charges are then introduced once again to restore the correct boundary conditions at the tip-vacuum, vacuum-C_{60}, and C_{60}-metal interfaces. The resulting potential at molecule i is U_i^{tip}. Finally, we also include the image potential of an electron (in the LUMO) or a hole (in the HOMO) in the tip, obtaining slightly different tip potentials for electrons and holes. U_i^{image} only depends on the layer index i, while U_i^{tip} also has a strong lateral dependence and is assumed to be localized to an area that would encompass about 100 C_{60} molecules per layer.

The work function for a multilayer C_{60} film on polycrystalline Ag is 4.68 eV[33] and for Au it is 5.26 eV.[34] These values are used to construct and approximate the potential between the C_{60}-Ag(111) sample and the Au tip. The difference between these work functions is 0.58 eV. While this difference is sensitive to Ag atoms coating the Au tip during the experimental tip preparation, this effect is not taken into account because the qualitative features of the resulting calculations are relatively insensitive to this difference. Thus, when the bias U is applied, we simply require that $U_t = U + 0.58\ \text{eV}$.

The tight-binding band gap of C_{60} is 2.24 eV, reasonably close to the experimental result 2.3 eV.[38] We have then applied a small correction to the C_{60} HOMO band, ΔE_g = - 0.06 eV. This approach puts the bottom of the LUMO band for the four layer system at about 0.27 eV, slightly above $E_F^S = 0$. This

alignment to E_F^S is arbitrary, but leads to a LUMO bound state going through E_F^S for approximately correct biases for one to four layer systems.

For a bias of $U < -3.32$ V, a split-off LUMO state moves below E_F^S and can be occupied. If this split-off state has the weight q_i on molecule i, we add these charges to the center of the molecule and calculate their images in the surfaces. This leads to an additional potential, U_i^{filled}, resulting from all the charges q_i and their images, except that the potential at molecule i from charge q_i is $q_i U_{\text{eff}}$. Here, $U_{\text{eff}} = 1.3$ V is an effective Coulomb interaction.[39] This calculated value has been shown to be in good agreement with experiment.[38] If the split-off state is assumed to be localized on one molecule in the outermost layers, the net effect of U_{eff} and the corresponding image charges is an overall shift of 1.5 V, comparable with the experimental value 1.6 V.[38]

The resulting Hamiltonian is then $H = H_0 + U$ with

$$H_0 = \sum_{i\nu\sigma} \varepsilon_{i\nu} \hat{n}_{i\nu\sigma} + \sum_{i\nu j\mu\sigma} t_{i\nu j\mu} \left(\hat{c}_{i\nu\sigma}^{\dagger} \hat{c}_{j\mu\sigma} + \hat{c}_{j\mu\sigma}^{\dagger} \hat{c}_{i\nu\sigma} \right)$$

$$U = \sum_{i\nu\sigma} U_{i\nu}^{\text{tip}} \hat{n}_{i\nu\sigma},$$

Here $\varepsilon_{i\nu} = \varepsilon_{i\nu}^0 + U_i^{\text{image}}$ for $\nu = 1, \cdots, 5$ $\left(\varepsilon_{i\nu} = \varepsilon_{i\nu}^0 - U_i^{\text{image}} \text{ for } \nu = 6,7,8 \right)$ is the position of the HOMO (LUMO) level for molecule i. $U_{i\nu}^{\text{tip}}$ has a ν dependence, since the image potential has different signs for electrons and holes. $\hat{c}_{i\nu\sigma}^{\dagger}$ and $\hat{c}_{i\nu\sigma}$ are the creation and annihilation operators for an electron in orbital ν with spin σ on molecule i, and $\hat{n}_{i\nu\sigma} = \hat{c}_{i\nu\sigma}^{\dagger} \hat{c}_{i\nu\sigma}$. $t_{i\nu j\mu}$ is the hopping integral between orbital ν on molecule i and orbital μ on molecule j. If one split-off LUMO state is filled, we also add the potential U_i^{filled} from the electron in this state.

Numerical Methods

The electronic structure is calculated using a Green's function technique. First the unperturbed Green's function $G_{i\nu j\nu'}^0(\varepsilon)$ as a function of energy ε is calculated for a film with an infinite lateral extension, taking the laterally periodic terms H_0 (and U_i^{image}) into account. Then we solve the Dyson equation for the perturbed Green's function $G_{i\nu j\nu'}(\varepsilon)$ where

$$G_{iνjν'}(\varepsilon) = G^0_{iνjν'}(\varepsilon) + \sum_{kν''} G^0_{iνkν''}(\varepsilon) \cdot U^{\mathrm{tip}}_{kν''} \cdot G_{kν''jν'}(\varepsilon)$$

We assume that the tip potential is non-negligible over N_{pert} molecules. Thus, the equations describing $G_{iνjν'}(\varepsilon)$ involves $\left(8N_{\mathrm{pert}}\right) \times \left(8N_{\mathrm{pert}}\right)$ matrices, where the factor 8 again originates from the frontier orbitals of C_{60}. The density of states (DOS), $N_{iν}(\varepsilon)$, projected on an orbital $iν$ is then

$$N_{iν}(\varepsilon) = \frac{1}{\pi} \mathrm{Im}\, G_{iνiν}(\varepsilon - i0^+)$$

where 0^+ is an infinitesimal positive quantity. The DOS has contributions both inside the C_{60} HOMO and LUMO bands as well as from split-off states outside of these bands.

Electronic structure

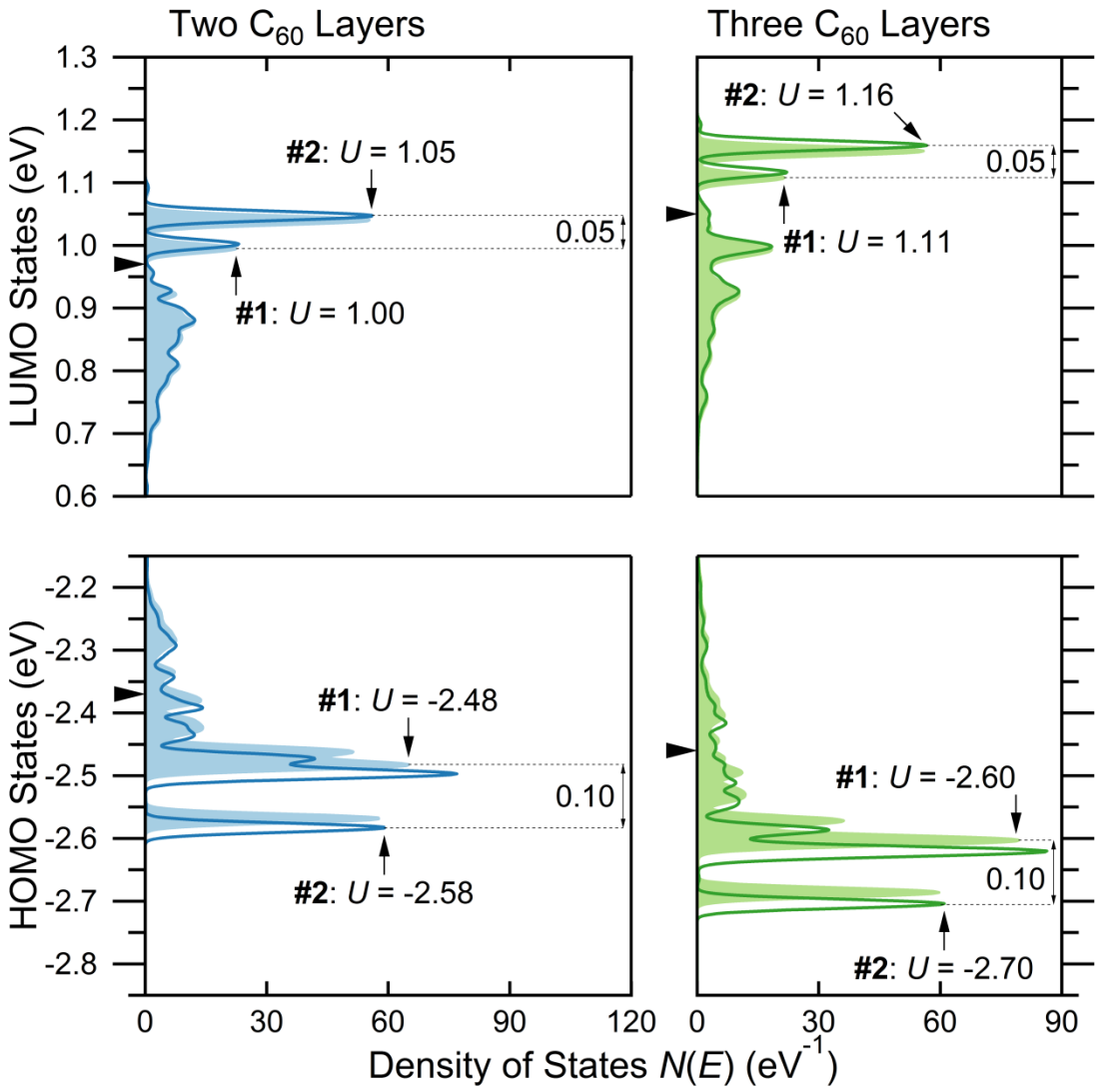

Supporting Figure 1. Calculated total density of states for two and three C_{60} layers at the labeled bias values *U* and tip distance *d* = 0.4 nm. The filled and unfilled curves represent the density of states at the onset bias *U* where tunneling through the first (#1) and second (#2) split-off state is possible, with the specific threshold *U* values indicated beside the arrows. The voltage differences between the two split-off states for each calculated system are indicated with double arrows. All features are broadened with a FWHM Lorentzian of 0.02 eV.

Supporting Figure 1 shows the electronic structure of the HOMO and LUMO bands for two and three C_{60} layers. These structures were calculated for values of U for which tunneling from a new split-off state or narrow resonance becomes possible. As a specific example, in order to tunnel through the first HOMO split-off state for 3 layers of C_{60}, an applied bias of -2.60 V is required. The curve that is labeled with "#1: -2.60" corresponds to the calculated density of states for an applied bias of -2.60 V. These values of U then correspond to structures in the dI/dU curves in Figure 3d. The positions of the structures agree well with experiment, except that the splitting between the peaks in the LUMO (and perhaps the HOMO) is too small compared with experiment (see Figure 3d in main text). This could be due to the neglect of crystal-field splittings in the model, specifically, the splitting of the t_{1u} and h_u states due to the presence of a surface, and the applied potential having a different effect on each orbital because they are oriented differently with respect to the tip and surface. In addition, the tunneling matrix elements may coincidentally cause some features to be obscured during measurements.

Qualitative behavior of HOMO and LUMO States in Figure 5 at small bias

As stated in the main text: "When a small bias is applied with a tip (-0.68 V in Figure 5b), the band edges stay fixed while the local DOS on the C_{60} directly below the tip is depleted at the upper band edge and accumulates at the lower edge. This causes the first moment to move to a lower potential, in this case, towards E_F^S (Figure 5a-b). This is due to the combined effects of the electrostatic and image potentials from the tip."

For the HOMO these contributions have opposite signs which happen to shift the HOMO slightly upwards.

The absolute energy shift of the density of states depends on both the electrostatic potential and the image potential, and their relative magnitudes. For Ag(111)-C_{60} it is the case that the HOMO DOS shifts positively in energy, in an opposite direction to the small negatively applied bias of -0.68 V.

Control experiment

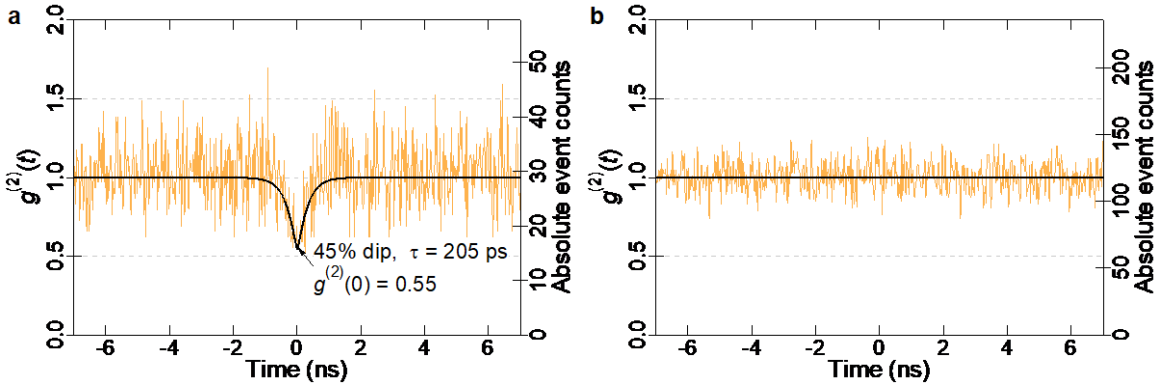

Supporting Figure 2. Photon intensity correlation dip (a) present on the C_{60} layers, and (b) absent on Ag(111). Same tip used in both measurements, -3.5 V, 250 pA. Absolute event counts is the total number of events per bin, each bin being 24.4 ps.

Tip-sample distance dependence of $g^{(2)}(t)$

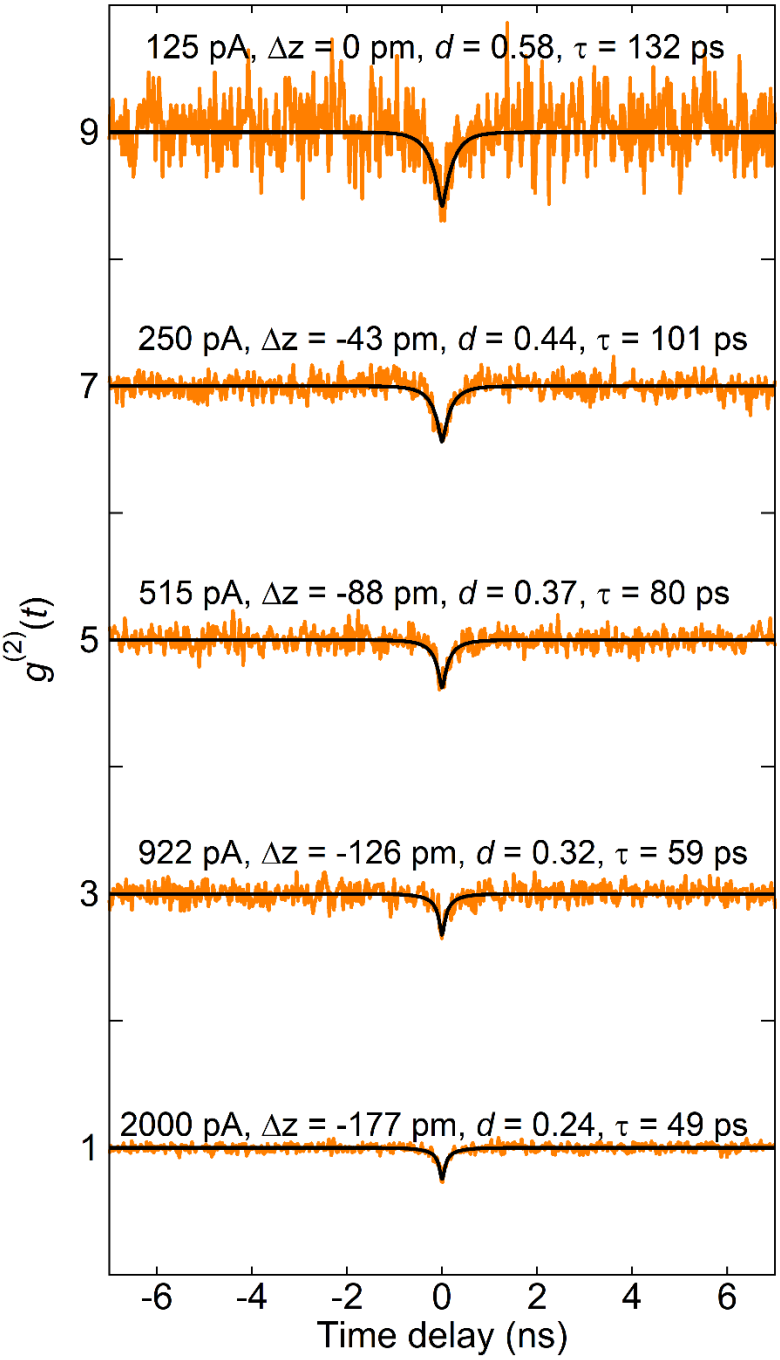

Supporting Figure 3. Photon intensity correlation function $g^{(2)}(t)$ as a function of tip-sample distance, measured with the same tip for fixed bias -3.5 V. Correlation functions were measured at the same position as in Figure 2c of the main text, vertically offset by multiples of 2 for clarity. The top trace is identical to Figure 2c. From top to bottom, the tip is repositioned by the relative distance Δz indicated in the plot. Resulting dip depths $d = 1 - g^{(2)}(0)$ and recovery time constants τ as indicated. The values of τ decrease for increasing current and increasing electric field in the C_{60} layer.

Bias dependence of $g^{(2)}(t)$

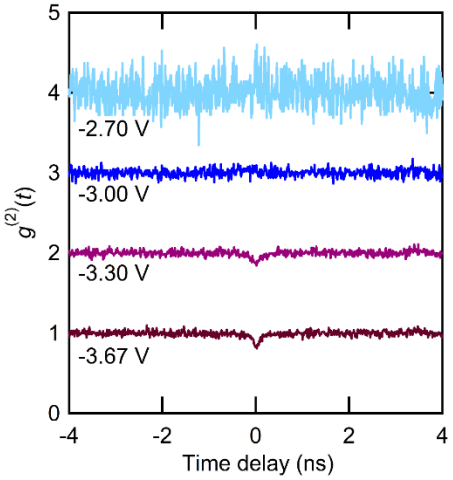

Supporting Figure 4. Photon intensity correlation function $g^{(2)}(t)$ as a function of bias tuned through the onset of split-off states, I = 2 nA. Traces vertically offset in units of 1 for clarity.

Differential conductance (dI/dV) spectra for 4-7 ML C_{60}

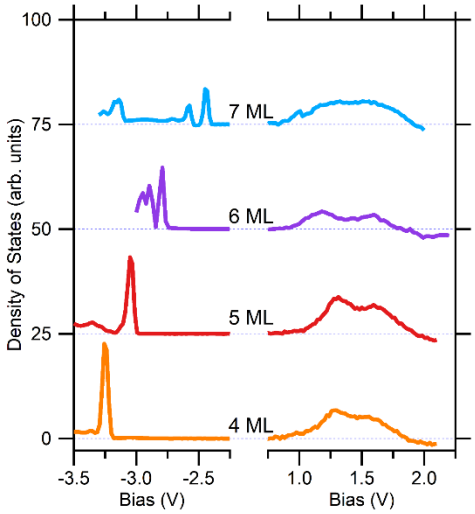

Supporting Figure 5. Differential conductance (dI/dV) spectra of 4-7 ML C_{60} atop Ag(111). Starting voltage setpoints of -3.5 V, -3.5 V, -3.0 V, and -3.3 V respectively, at I = 100 pA. The intensities of the features between 0.5 V and 2.5 V are multiplied by a factor of 10. The 4 and 5 ML traces are identical to those shown in Figure 3 of the main text.